



Electrical-driven self-heat recuperative pressure-swing azeotropic distillation to minimize process cost and CO₂ emission: Process electrification and simultaneous optimization

Chengtian Cui ^a, Nguyen Van Duc Long ^b, Jinsheng Sun ^{a,*}, Moonyong Lee ^{b,**}

^a School of Chemical Engineering and Technology, Tianjin University, Tianjin, 300072, PR China

^b School of Chemical Engineering, Yeungnam University, Gyeongsan, 712-749, South Korea



ARTICLE INFO

Article history:

Received 4 November 2019

Received in revised form

10 January 2020

Accepted 17 January 2020

Available online 20 January 2020

Keywords:

Self-heat recuperation

Pressure-swing

Azeotropic distillation

Simultaneous optimization algorithm

Thermal-electric integration

ABSTRACT

Azeotropic separation by pressure-swing distillation (PSD) is one of the most costly processes in the chemical industry. To minimize process cost and CO₂ emission, process electrification based on self-heat recuperation technology (SHRT) has been implemented in many thermal-driven processes. Enlightened by these facts, a novel electrical-driven PSD-SHRT process is proposed and compared with conventional thermal-driven PSD (PSD-CONV) and PSDs integrated with heat integration and heat pump. Two typical binary systems – tetrahydrofuran (THF)/water with minimum-boiling azeotrope and acetone/chloroform with maximum-boiling azeotrope – are selected to investigate the potential economic and environmental benefits of process electrification. To make a fair comparison, all the processes are optimized to a minimum in total annualized cost (TAC) based on a simulation-based optimization framework combining Aspen Plus (process simulator) and MATLAB (external optimizer). The optimization results indicate PSD-SHRT to be the lowest in both TAC and CO₂ emission of all the alternative processes. In THF/water system, PSD-SHRT triumphs over PSD-CONV by 23.72% in TAC and 83.67% in CO₂ emission, respectively. Corresponding values increase to 47.82% and 92.90% in the acetone/chloroform system. These improvements verify the significant advantages of process electrification and also encourage more orientations to introduce SHRT into other processes.

© 2020 Elsevier Ltd. All rights reserved.

1. Introduction

Chemical industries have for long been consuming a huge amount of fossil fuel as heat sources for unit operations, contributing to major emission of CO₂, the infamous greenhouse gas, into the atmosphere. Consuming more than 50% of the plant operating cost, distillation is a mature thermal-driven separation technology widely used in the chemical industry [1]. This large amount of energy consumption makes any improvements in distillation to bring about significant benefits. That is, any research thrust in distillation processes will be highly welcomed to reduce process costs when satisfying product requirements and relieving environmental burden as well. As industry fully recognizes this public concern on environmental impact, it turns to all possible measures

of higher efficiency, such as cleaner electricity, for plant sustainability and global warming suppression [2]. Since electricity can be generated from sustainable energy sources (wind, solar, etc.), pursuing energy-efficient process electrification is a promising way to develop more sustainable chemical processes.

Azeotropes are one of the difficulties frequently encountered in distillation design. Amongst the strategic proposals, pressure-swing distillation (PSD) is advantageous over those requiring a third component to shift vapor-liquid equilibrium (VLE) and contaminate one of the products [3], such as extractive and heterogeneous azeotropic distillations. PSD, the target of this work, with a prerequisite for the feeding components to be pressure-sensitive, is achieved with a high-pressure column (HPC) and a low-pressure column (LPC) [3]. Naturally, the pressure difference between two columns facilitates double-effect heat integration (DEHI) [4–7]. Besides, heat pump assisted distillation (HPAD) is also ready for lower energy consumption and better profitability [8–11]. Despite the heightened distillation energy efficiency through DEHI and HPAD options, an inefficient sequential design approach should

* Corresponding author.

** Corresponding authors.

E-mail addresses: jssun2006@vip.163.com (J. Sun), mynlee@yu.ac.kr (M. Lee).

Nomenclature	
<i>Acronyms</i>	
AOT	annual operating time
BF	bottom flash
CAPEX	capital expenditure
COP	coefficient of performance
CSCC	cold stream composite curve
DEHI	double-effect heat integration
EO	equation-oriented
FHI	full heat integration
FSR	feed split ratio
GCC	grand composite curve
HPAD	heat pump assisted distillation
HPC	high-pressure column
HSCC	hot stream composite curve
LMTD	logarithmic mean temperature difference
LPC	low-pressure column
MVR	mechanical vapor recompression
OPEX	operational expenditure
PCS	pre-compressor splitting ratio
PHI	partial heat integration
PSD	pressure-swing distillation
SHRT	self-heat recuperation technology
TAC	total annualized cost
T-H	temperature-enthalpy
THF	tetrahydrofuran
VC	vapor compression
VLE	vapor-liquid equilibrium
WHR	waste heat recovery
<i>Roman letters</i>	
A	heat transfer area
B	bottom product mole flow rate
C	cost
D	distillate mole flow rate
D _c	column diameter
f	annualization factor
H _c	column height
N	stage number
NF	feed stage number
NT	total stage number
P	pressure
Q	heat duty
RR	reflux ratio
T	temperature
W	electrical power
x	mole composition

not be omitted as another obstruction for lowering process cost [12,13]. This happens in traditional design approaches only maximizing heat recovery from a fixed set of process streams from and to distillation columns via pinch analysis after determining all column decision variables [14]. However, the process stream conditions (flow rates, temperatures, etc.) are usually in high conjunction with the column specifications. For example, in a DEHI process, preheating the LPC feed can decrease its reboiler duty, which might further affect the reflux ratio of HPC. Therefore, such a hierarchical approach is unable to reflect the interactions between distillation and heat integration, resulting in failures to reach an optimum design [12,13]. The drawback of the sequential design approach calls for a simultaneous optimization method considering the distillation system and heat integration as two trade-off aspects within a single synthesis problem [15].

To date, the concept of self-heat recuperation technology (SHRT) has been used in various thermal-driven processes, contributing to considerable energy-saving since its proposal by Kansha et al. [16]. Usually, in the temperature-enthalpy (T-H) diagram, the movements of hot and cold stream composite curves (HSCC and CSCC) in pinch analysis are limited in only horizontal direction within a certain range of temperatures. While for SHRT in the same scenario, the HSCC can be shifted vertically through adiabatic compression in the T-H diagram. This way it is possible to re-circulate the whole process heat without any extra heat addition, so the whole process can be driven by electricity. In the design of a distillation column, SHRT can be regarded as a further improvement of HPAD. HPAD usually considers only latent heat when using compressed vapor to drive the column reboiler, neglecting the extra sensible heat for preheating, also, in contrast, recovered by the SHRT. Recently, SHRT have demonstrated significant energy-saving potentials in various industrial distillation-based processes, such as natural gas liquid recovery [17], aromatics separation [18], crude distillation [19], biodiesel production [20], cryogenic air separation [21], acid gas removal [22], bioethanol dehydration [23], etc. Great advantageous as SHRT has been in energy-saving, it was achieved on the old track

of sequential design approach, namely, synthesizing the distillation system and heat integration separately. Specifically, in this area, Xia et al. [24] applied SHRT in PSD separating minimum-boiling isopropyl alcohol/di-isopropyl ether system through a sequential design approach. The authors first designed a PSD process and then added heat integration based on pinch analysis, with column pressures non-optimized. Since many authors [25–27] has pointed out the importance of optimizing column pressure, the separation of isopropyl alcohol/di-isopropyl ether system still leaves rooms for further improvement if all the important decision variables, especially the column pressures, could be optimized. On the other hand, the sequential approach ignoring the interaction between distillation and heat integration may not get the whole process fully optimized [27]. This scenario inspires investigation into a simultaneous approach for a fair trade-off between interactive column inside operation and its background heat recovery. However, such a simultaneous optimization method has by far rarely been documented in SHRT-based distillation processes. The published resources of similarity include Christopher et al. [28] for propylene/propane and Li et al. [29] for ethylbenzene/styrene. Both works have demonstrated great profitability of integrating SHRT compared to the conventional column. However, propylene/propane and ethylbenzene/styrene are insensitive to pressure, so the advantage of optimizing column pressure is marginal [26]. Unlike pressure-insensitive components, azeotropes to be separated by PSD must be sensitive to pressure, so any changes in pressure will transfer effects to process stream conditions, unit operations, and eventually the whole process. Besides, compared to the single column with SHRT, the involvement of more columns in PSD dramatically increases the number of decision variables. In this work, we extend the concept of SHRT to the PSD, with simultaneous optimization instead of the traditional sequential design approach, to obtain an optimum design.

Generally speaking, the current simultaneous optimization mainly includes two pathways – equation-oriented (EO) and simulation-based optimizations. The former relies on optimization

models developed in EO modeling environment such as GAMS, while the latter usually applies a commercial process simulator together with an external optimizer. Because PSD involves the azeotropic system of strong non-ideal VLE behaviors and complicated MESH (mass, equilibrium, summation, and heat) equations describing distillation columns, the simulation-based optimization is advantageous over the EO optimization approach in complicated process simulations. This preponderance attributes to implementing high-accuracy thermodynamic libraries and high-fidelity unit operation models [15]. Therefore, a simulation-based optimization framework that connects Aspen Plus (process simulator) and MATLAB (external optimizer) is developed in this study. The Aspen Plus process configurations are developed in the rigorous environment. Since the process models in Aspen Plus can be regarded as a large black box unready for derivative information, a derivative-free stochastic algorithm written in MATLAB is utilized to optimize the overall process system.

When the methodology is ready, synthesis can be conducted of a novel electrical-driven self-heat recuperative PSD with all decision variables simultaneously optimized. To evaluate the performance of the proposed PSD-SHRT, alternative processes, including the PSD-CONV (conventional PSD), PSD-DEHI, and PSD-HPAD, will be compared under the same objective function. Since PSD can be applied to both minimum-boiling and maximum-boiling pressure-sensitive azeotropes, two typical binary systems – tetrahydrofuran (THF)/water with minimum-boiling azeotrope and acetone/chloroform with maximum-boiling azeotrope – are considered as case studies to demonstrate the potential economic and environmental benefits of process electrification based on SHRT.

2. Process design and evaluation

2.1. Azeotropic systems

2.1.1. Minimum-boiling THF/water system

To perform a fair comparison of the PSD-CONV, PSD-DEHI, PSD-HPAD, and PSD-SHRT, the crude feed is 2000 kmol/h 6/94 mol% THF/water at 30 °C [30,31]. The purity demands for THF and water are 99.99 mol% and 99.999 mol%, respectively. Wilson equation is used as the thermodynamic model in Aspen Plus, and the built-in binary interaction parameters are given in Table 1. According to Abu-Elshah and Luyben [30] and Luyben [31], in the PSD-CONV and PSD-DEHI for THF/water separation, the pressures of LPC and HPC were set at 0.465 and 11.3 bar, respectively. These pressures are used in the corresponding T-x-y and x-y diagrams as given in Fig. 1, in which the distillate and bottoms compositions are referred to Luyben's work [31]. These diagrams tell that the crude feed must first enter the LPC to jump over the azeotropic composition. This thermodynamic insight is used to guide the concept design of the following process configurations.

Table 1
Binary interaction parameters for THF/water and acetone/chloroform systems.

Thermodynamic model	Wilson model	UNIQUAC model
Component i	THF	Acetone
Component j	Water	Chloroform
A _{ij}	-9.44727	-1.0178
A _{ji}	1.11992	1.2757
B _{ij}	2110.94	535.401
B _{ji}	-847.796	-555.939
C _{ij}	0	0
C _{ji}	0	0

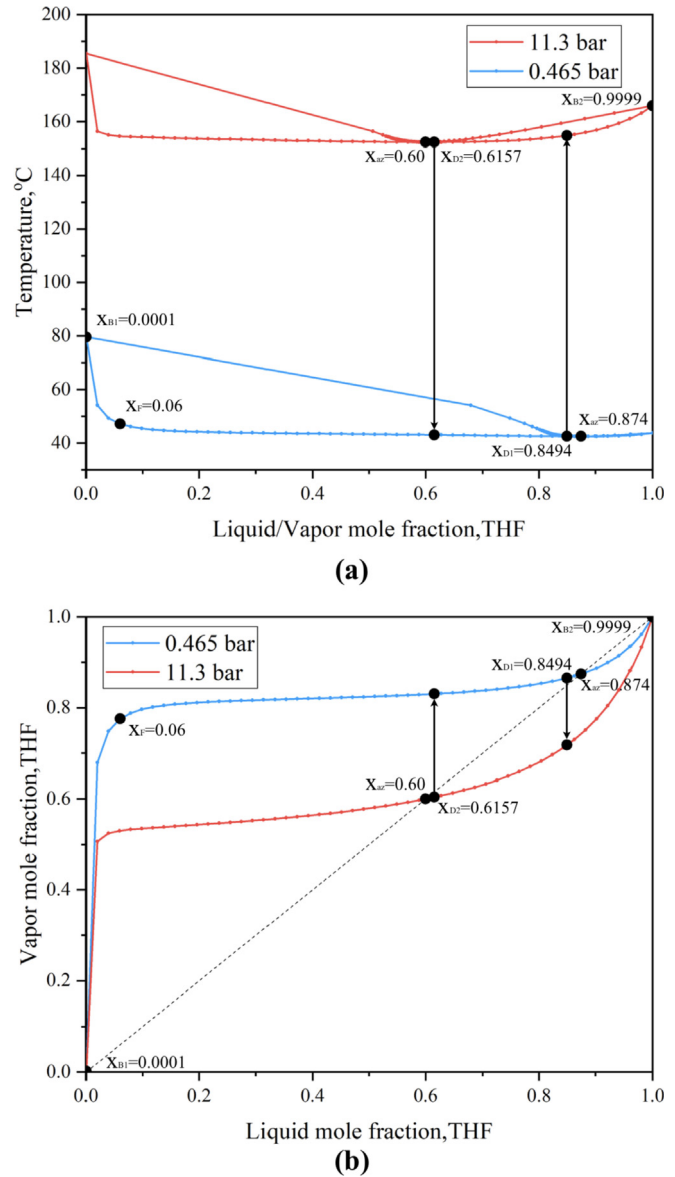


Fig. 1. (a) T-x-y diagram of THF/water and (b) x-y diagram of THF/water at 0.465 bar and 11.3 bar.

2.1.2. Maximum-boiling acetone/chloroform system

Fig. 2 gives the T-x-y and x-y diagrams for this system at 0.77 and 10 bar, with the marked compositions from Luyben's work [32]. The small azeotropic composition shift with changing pressure and the close-boiling nature between the two components indicate the high separation difficulty by PSD, requiring more separation stage and large recycle flow rate. To make a comparison, the fresh feed and product target are identical to the previous work [32] – flow rate is 100 kmol/h of 50/50 mol% acetone/chloroform at 47 °C and the desired product purification is 99.5 mol% for each component. UNIQUAC thermodynamic model is used in Aspen Plus with the built-in parameters given in Table 1. The thermodynamic diagrams (Fig. 2) inspire that the fresh feed has to be first added to the HPC to achieve the desired separation.

2.2. Process configurations

Four process configurations – PSD-CONV, PSD-DEHI, PSD-HPAD,

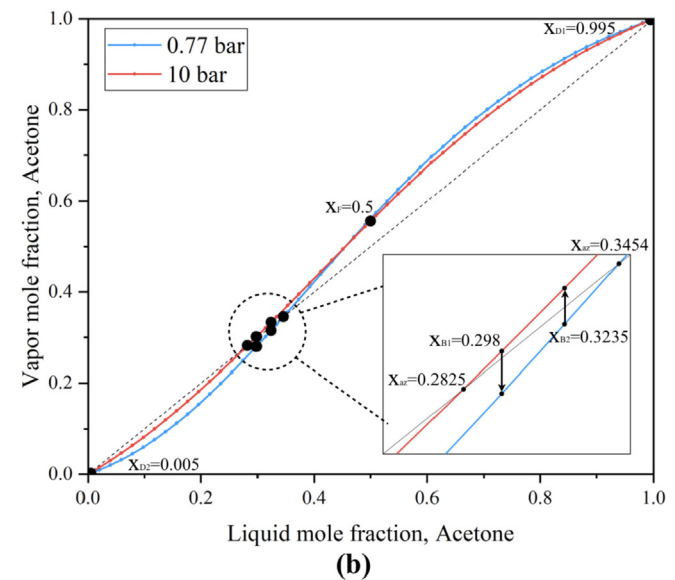
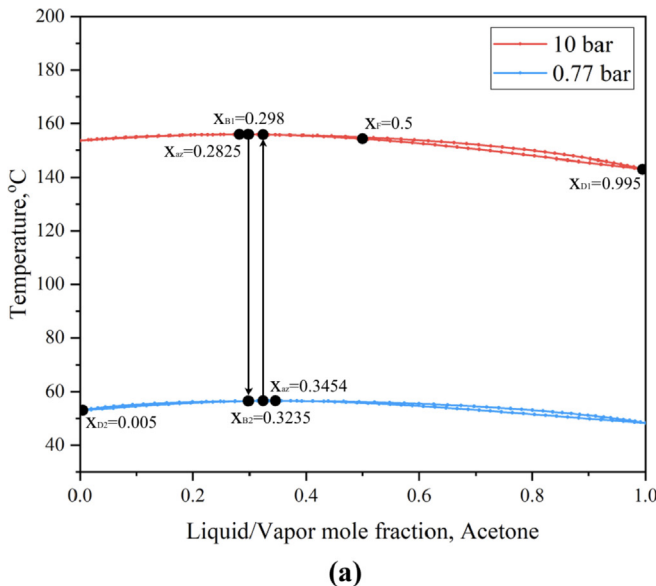


Fig. 2. (a) T-x-y diagram of acetone/chloroform and (b) x-y diagram of acetone/chloroform at 0.77 bar and 10 bar.

and PSD-SHRT – are considered for the separation comparisons of THF/water and acetone/chloroform systems. For different azeotrope types (minimum-boiling or maximum-boiling) with various feed compositions, the distillation sequence can be conceptually determined by **T-x-y** and **x-y** diagrams. In this section, all the process configurations for the two systems are provided to illustrate their differences. Although the process configurations differ from azeotrope types, the common features of designing a distillation system are identical – all discrete variables like feed location/total stage number and continuous variables like column pressure, reflux ratio, etc. have to be determined. Because of the involvement of both discrete and continuous variables, the optimization problem can be formulated as a mixed-integer nonlinear programming (MINLP). These decision variables are introduced as follows.

2.2.1. Configuration 1 – PSD-CONV

Figs. 3a and 4a present the PSD-CONV for THF/water and acetone/chloroform systems, respectively. For the minimum-

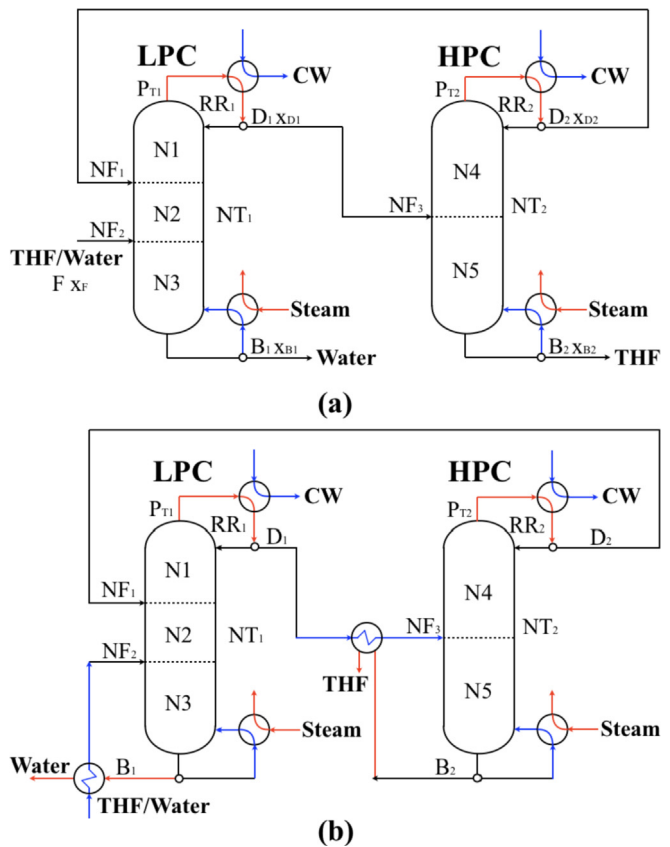


Fig. 3. Schematic diagrams of (a) PSD-CONV and (b) PSD-CONV with economizers for THF/water separation.

boiling THF/water system, the distillate is recycled while the feed flows through LPC and HPC in sequence, as conceptually demonstrated in Fig. 1. For the maximum-boiling acetone/chloroform system, the bottoms stream is recycled with HPC and LPC in sequence, as displayed in Fig. 2. As shown in Figs. 3b and 4b, economizers can be naturally added for feed preheating to recover the sensible heat from column effluents. This waste heat recovery (WHR) measure is also applied in the other process alternatives.

For the PSD-CONV, the discrete variables include feed location (NF₁, NF₂, and NF₃) and total stage number (NT₁ and NT₂). For an easy treatment of the discrete variables in simultaneous optimization, N1 to N5 are defined as the stage number in each column section, excluding condenser and/or reboiler. Therefore, the column structural parameters can be expressed as below:

$$NF_1 = N1 + 1 \quad (1)$$

$$NF_2 = N1 + N2 + 1 \quad (2)$$

$$NT_1 = N1 + N2 + N3 + 2 \quad (3)$$

$$NF_3 = N4 + 1 \quad (4)$$

$$NT_2 = N4 + N5 + 2 \quad (5)$$

Except for the discrete variables, the continuous variables involve the pressures (P_{T1} and P_{T2}) and reflux ratios (RR_1 and RR_2) in the two columns and the approach of the distillate compositions (x_{D1} and x_{D2}) or bottoms compositions (x_{B1} and x_{B2}) to the corresponding azeotropic compositions at these pressures. In

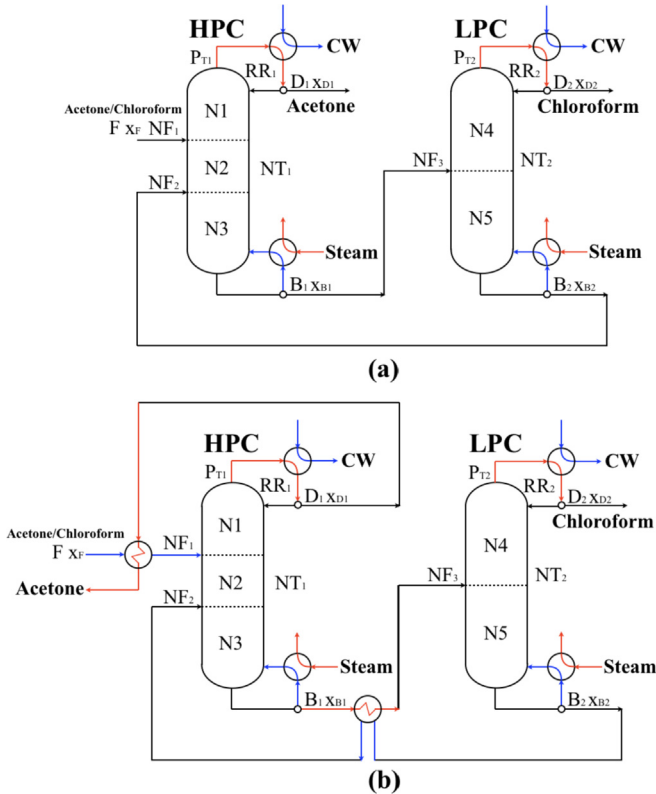


Fig. 4. Schematic diagrams of (a) PSD-CONV and (b) PSD-CONV with economizers for acetone/chloroform separation.

simultaneous optimization, treating distillate and bottoms compositions as decision variables can cause convergence issues, because their boundaries are strongly dependent on the column pressures and structural parameters. To circumvent the optimization difficulties, the recycle flow rate (D_2/B_2) is selected as the decision variable as it strongly depends on the difference between the distillate/bottoms compositions [30].

Therefore, a totally of 10 decision variables should be provided, including five discrete variables (N1-N5) and five continuous variables (P_{T1} , P_{T2} , RR_1 , RR_2 , and D_2/B_2). All these decision variables are marked in Figs. 3 and 4.

2.2.2. Configuration 2 – PSD-DEHI

The basic principle of DEHI is HPC overhead vapor to drive the LPC reboiler. As a PSD naturally has an HPC and an LPC, it is convenient to apply this WHR measure. DEHI can be classified as full and partial heat integrations (FHI and PHI). If the heat duties in the two columns are perfectly matched, an FHI between the two columns can be achieved. If not, an auxiliary reboiler should be added to compensate for the extra heat duty. The PSD-DEHIs with economizers for THF/water and acetone/chloroform systems are demonstrated in Figs. 5 and 6, respectively. The degree of PHI depends on simultaneous process optimization. When the duty of the auxiliary reboiler approaches to zero, the PHI is reduced to an FHI.

The decision variables for PSD-DEHI are identical to the PSD-CONV, including stage number in each section (N1-N5), column pressures (P_{T1} and P_{T2}), reflux ratios (RR_1 and RR_2), and recycle stream (D_2 or B_2).

2.2.3. Configuration 3 – PSD-HPAD

In a conventional distillation column, the high-temperature heat is supplied at the reboiler by a hot utility and a similar

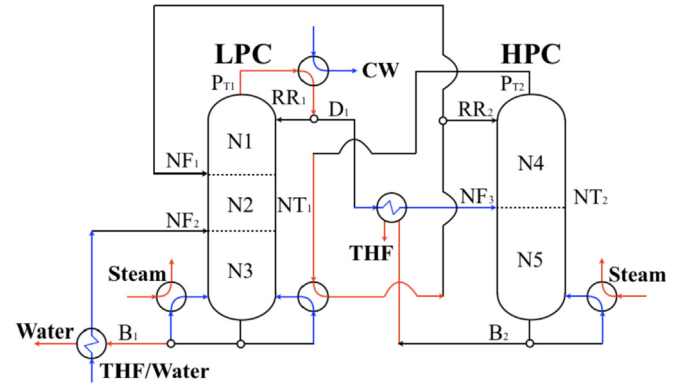


Fig. 5. Schematic diagram of PSD-DEHI for THF/water separation.

amount of low-temperature heat is wasted to a cold utility at the condenser, resulting in a substantial energy degradation [8]. Heat pump can upgrade the waste heat at the condenser to drive the reboiler, substantially reducing the overall energy consumption. So far, many types of heat pumps have been found in practical distillation applications [8]. The most commonly used are the absorption heat pump and mechanical heat pump. The mechanical heat pump is categorized into three types – vapor compression (VC), mechanical vapor recompression (MVR), and bottom flash (BF) [33]. Of the aforementioned types, the MVR has gained more recognition due to its outstanding benefits [34]. Therefore, MVR is considered to assist the PSD in the present study. Figs. 7 and 8 show PSD-HPAD with economizers for THF/water and acetone/chloroform separations, respectively. If the upgraded heat is not sufficient for driving the column, an auxiliary reboiler is ready to make up. During the compression process, partial saturated vapor might be condensed in the compressor, which can damage the compressor. In this case, an optional preheater driven by the steam utility is added at the suction of the compressor to superheat the vapor. So the degree of superheating (T_{sup}) should be treated as a decision variable in the optimization. If the degree of superheating is zero, a compressor preheater is unnecessary. Likewise, partial saturated liquid might be flashed during the expansion, so an auxiliary condenser is added after the valve. Another important decision variable is the compressor discharge pressure (P_C), which determines the outlet state of the compressed vapor and the required power for the compressor.

The total 14 decision variables for the PSD-HPAD include stage number in each section (N1-N5), column pressure (P_{T1} and P_{T2}), reflux ratios (RR_1 and RR_2), recycle stream (D_2 or B_2), degrees of superheating (T_{sup1} and T_{sup2}), and compressor discharge pressures (P_{C1} and P_{C2}).

2.2.4. Configuration 4 – PSD-SHRT

In previous PSD-HPAD, only latent heat of the compressed vapor is utilized while the sensible heat is wasted in the condenser. While in the conventional SHRT column (Fig. 9a) proposed by Matsuda et al. [18], both the latent and sensible heat are re-circulated in the process by using compressor and economizer. Since the inlet feed is heated by both the compressed vapor and bottoms, an additional decision variable – feed split ratio (FSR) – should be involved to satisfy the preheating temperature range. Herein, the FSR is defined as the flow rate of stream 1/the overall flow rate of streams (1 + 2) (Fig. 9a). In the original work [18], the vapor was not condensed during compression so there is no compressor preheater. However, we suggest to add an optional preheater to avoid condensation herein. Considering the defects of the conventional SHRT, a

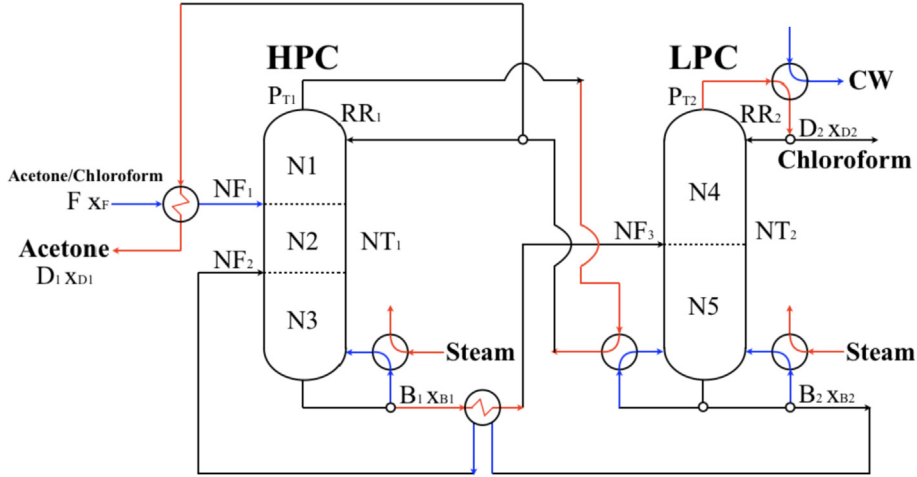


Fig. 6. Schematic diagram of PSD-DEHI for acetone/chloroform separation.

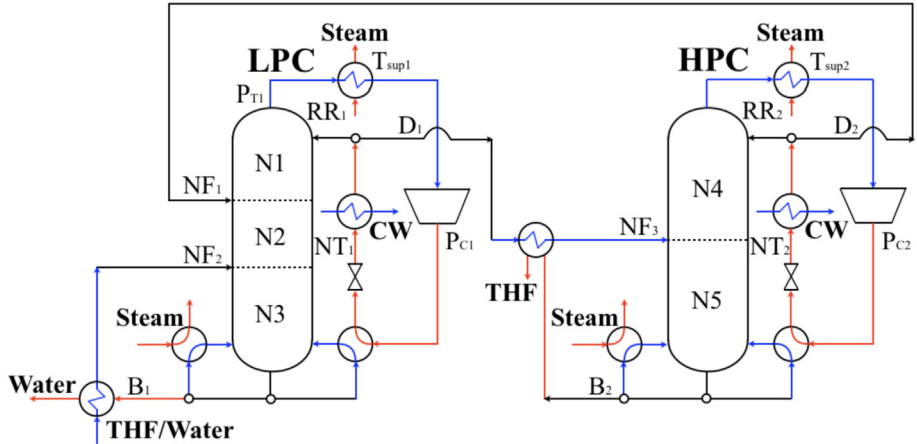


Fig. 7. Schematic diagram of PSD-HPAD for THF/water separation.

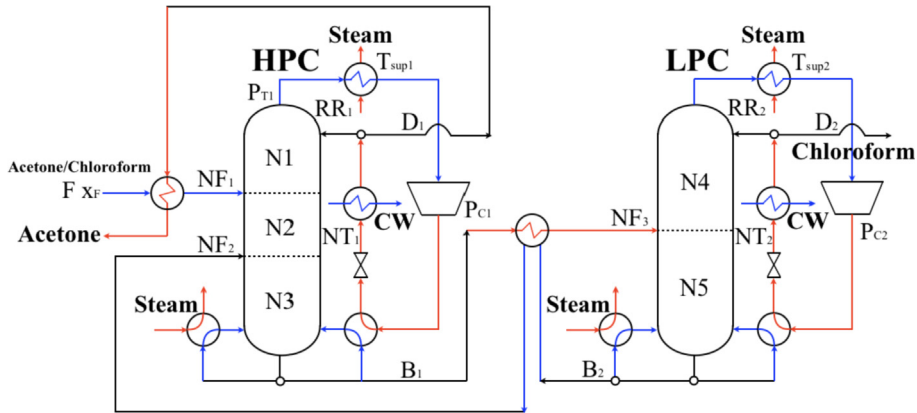


Fig. 8. Schematic diagram of PSD-HPAD for acetone/chloroform separation.

modified SHRT structure (Fig. 9b) is proposed involving pre-compressor splitting, compressor inlet preheating, and feed pre-heating, in which the pre-compressor splitting ratio (PCS) is defined as the flow rate of stream 1/the overall flow rate of streams (1 + 2) (Fig. 9b). Through the stream bypass measure, it is possible to reduce the compressor cost. This modified SHRT is extended to

the PSD process in this work.

In the conventional SHRT column exemplified by an aromatic separation process, all the feed and products were set at standard conditions (25 °C and 0.10 MPa), allowing the feed preheating by the bottoms [18]. However, in the synthesis of PSD-SHRT, it is not always possible to preheat feed by compressed vapor as its

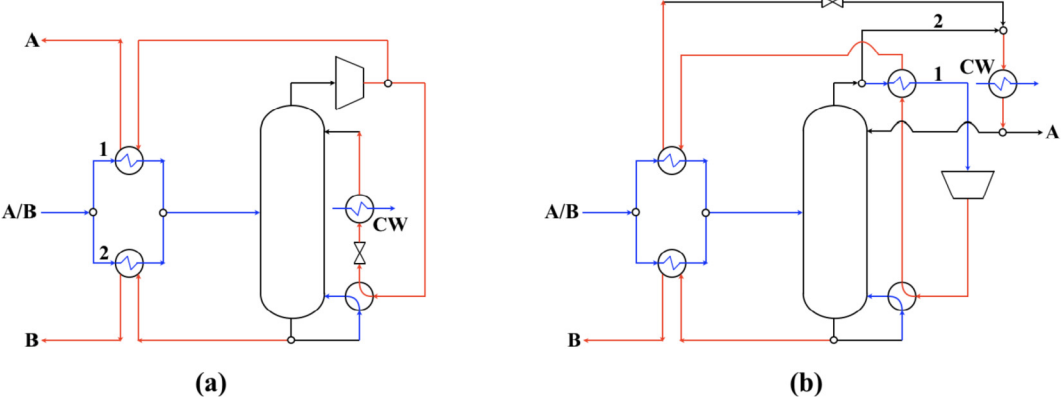


Fig. 9. Schematic diagrams of (a) the conventional SHRT column and (b) the modified SHRT column.

temperature might be too low. Therefore, for each specific azeotropic system, the synthesis of PSD-SHRT should refer to its base HPAD design.

Fig. 10 demonstrates a PSD-SHRT for THF/water separation. Since the THF/water crude feed temperature (30°C) is much lower than the column temperature profile, feed preheating by compressed vapor and bottoms can eventually lower reboiler duty. Likewise, the HPC inlet feed is preheated before entering the column. Of course it is also possible to preheat the HPC inlet feed by HPC distillate, but since the sensible heat from the HPC distillate is very small, it is therefore not considered for further preheating. The total 18 decision variables are stage number in each section (N1-N5), column pressures (P_{T1} and P_{T2}), reflux ratios (RR_1 and RR_2), recycle stream flow rate (D_2), feed split ratios (FSR_1 and FSR_2), pre-compressor splitting ratios (PCS_1 and PCS_2), degrees of super-heating ($T_{\text{sup}1}$ and $T_{\text{sup}2}$), and compressor discharge pressure (P_{C1} and P_{C2}).

Fig. 11 shows the schematic diagram of PSD-SHRT for acetone/chloroform separation. In this process, the HPC inlet feed is preheated and the LPC inlet feed is precooled for better column temperature profile matching, so there is no FSR design variable in this process. The total 16 decision variables for this case are stage number in each section (N1-N5), column pressures (P_{T1} and P_{T2}), reflux ratios (RR_1 and RR_2), recycle stream flow rate (B_2), pre-compressor splitting ratios (PCS_1 and PCS_2), degrees of super-heating ($T_{\text{sup}1}$ and $T_{\text{sup}2}$), and compressor discharge pressure (P_{C1} and P_{C2}).

and P_{C2}).

2.3. Process evaluation

2.3.1. Economic evaluation

Total annualized cost (TAC, US\$/a) is introduced as the economic indicator to evaluate different processes. TAC considers both operational and capital expenditures (OPEX and CAPEX):

$$TAC = OPEX + f \cdot CAPEX \quad (6)$$

where f is defined as the annualization factor, which is used to capitalize on the investment cost over the plant equipment lifetime [35]:

$$f = \frac{i \cdot (1+i)^n}{(1+i)^n - 1} \quad (7)$$

where i is fractional interest rate per year and n the lifespan of plant equipment. 0.1 and 20 years are used as the values of i and n , respectively.

OPEX (US\$/a) mainly includes hot utility (C_{hu}) for the reboilers, cold utility (C_{cu}) for the condensers, and electrical power (C_{elec}) for the compressors. An annual operating time (AOT) of 8000 h is used. Thus:

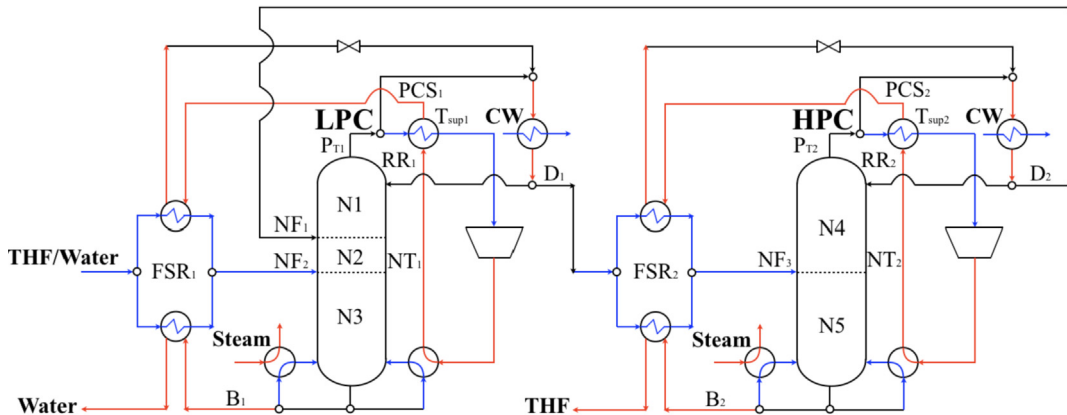


Fig. 10. Schematic diagram of PSD-SHRT for THF/water separation.

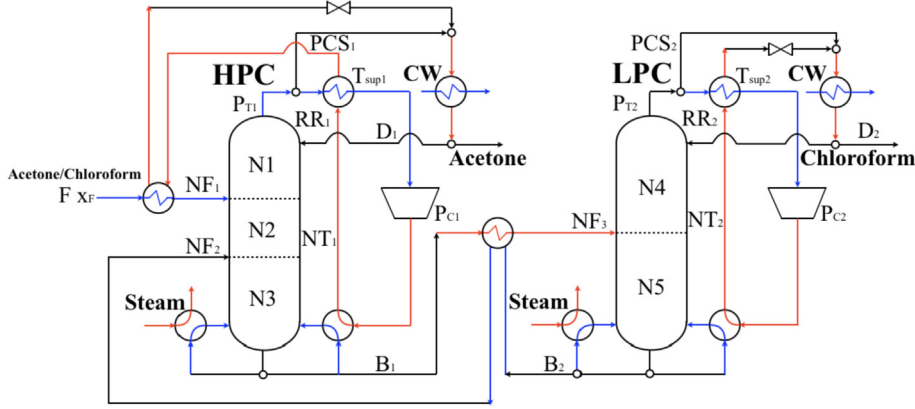


Fig. 11. Schematic diagram of PSD-SHRT for acetone/chloroform separation.

$$OPEX = AOT \cdot \left[\sum(C_{hu} \cdot Q_{hu}) + \sum(C_{cu} \cdot Q_{cu}) + \sum(C_{elec} \cdot W) \right] \quad (8)$$

where Q_{hu} , Q_{cu} , and W are the energy consumption of heating, cooling, and compression duty, respectively. The available utilities include low-pressure steam (LPS, 6 bar/160 °C), medium-pressure steam (MPS, 11 bar/184 °C), cooling water (30 °C–40 °C), and electrical power. The prices are 7.78, 8.22, 0.354, and 16.8 US\$/GJ, respectively [36].

The CAPEX (US\$) considers the distillation column (C_{COL}), tray (C_{TRAY}), heat exchanger (C_{HEX}), and compressor (C_{COM}). The costs of the pump, pipeline, and valve are neglected. Hence:

$$CAPEX = \sum(C_{COL} + C_{TRAY} + C_{HEX} + C_{COM}) \quad (9)$$

The CAPEX of the column shell (C_{COL} , US\$) and tray (C_{TRAY} , US\$) can be estimated from Ref. [36]:

$$C_{COL} = 17,640 \cdot D_c^{1.066} \cdot H_c^{0.802} \quad (10)$$

$$C_{TRAY} = 229 \cdot D_c^{1.55} \cdot (NT - 2) \quad (11)$$

The column diameter D_c (m) is calculated using the Aspen Tray Sizing option, in which sieve tray type with two passes is used for all column sections and a stage pressure drop of 0.007 bar is considered. The column height H_c (m) is estimated as below:

$$H_c = 1.2 \cdot 0.61 \cdot (NT - 2) \quad (12)$$

Without considering equipment details, the CAPEX of the heat exchanger (C_{HEX} , US\$) is estimated by its heat transfer area (A , m²) [36]:

$$C_{HEX} = 7,296 \cdot A^{0.65} \quad (13)$$

The heat transfer area is calculated based on:

$$A = \frac{Q}{U \cdot LMTD} \quad (14)$$

where Q is the heat duty, U the overall heat-transfer coefficient, and $LMTD$ the logarithmic mean temperature difference between the

hot and cold streams. The adopted overall heat-transfer coefficient for the condenser is 0.852 kW/(°C · m²), while for reboiler and process-to-process heat exchanger 0.568 kW/(°C · m²) [36].

The compressor cost (C_{COM} , US\$) is calculated as a function of the work done (W_c , kW) [36]:

$$C_{COM} = 9,560 \cdot W_c^{0.82} \quad (15)$$

In this work, the compressor mechanical/isentropic efficiency was set at 0.8/0.72.

2.3.2. Environmental evaluation

The CO₂ emission is introduced as an important environmental indicator to evaluate the environmental impact and sustainability of all the alternative processes. The CO₂ emission is generally related to the energy input in the process. Of which, the steam for reboiler is normally generated from the combustion of fossil fuel like coal, heavy fuel oil, and natural gas. The electrical power could be generated from either conventional fossil fuel or renewable energy sources such as wind, solar, biomass, etc. To simplify the calculation, heavy fuel oil is assumed for the steam used in reboiler, and the electrical power is provided by thermal sources.

Gadalla et al. [37] proposed a simple model for the computation of CO₂ emissions in the distillation process, which is given below:

$$[CO_2]_{emissions} = \left(\frac{Q_{Fuel}}{NHV} \right) \cdot \left(\frac{C\%}{100} \right) \cdot \alpha \quad (16)$$

where $\alpha = 3.67$ is the molar mass ratio of CO₂ and C. For heavy fuel oil, the net heating value (NHV) is 39771 kJ/kg and the carbon content C% is 86.5 kg/kg. Besides, the duty of the fuel (Q_{Fuel}) could be calculated as below:

$$Q_{Fuel} = \frac{Q_{Proc}}{\lambda_{Proc}} \cdot (h_{Proc} - 419) \cdot \frac{T_{FTB} - T_0}{T_{FTB} - T_{Stack}} \quad (17)$$

where Q_{Proc} (kJ) is the heat duty of the reboiler. λ_{Proc} (kJ/kg) and h_{Proc} (kJ) are the latent heat and the enthalpy of LPS or MPS, respectively. The boiler feed water is assumed to be at 100 °C with an enthalpy of 419 kJ/kg. $T_0 = 25^\circ\text{C}$ is the reference temperature, $T_{FTB} = 1800^\circ\text{C}$ the flame temperature, and $T_{Stack} = 160^\circ\text{C}$ the stack temperature.

Based on the steam tables in the book of Smith et al. [38], the

CO₂ emissions for LPS and MPS are 96.8 kg CO₂/GJ and 102 kg CO₂/GJ, respectively. On the other hand, the CO₂ emissions for electrical power are taken as 51.1 kg CO₂/GJ [39]. From the basic CO₂ emission data, it can be deduced that electrical-driven processes are much more environmentally benign than thermal-driven processes.

2.3.3. Heat pump performance evaluation

The coefficient of performance (COP) can be used to evaluate the heat pump performance in the distillation process. The COP is defined as:

$$COP = \frac{Q_h}{W} \quad (18)$$

where Q_h is upgraded heat rejected at high-temperature and W is the heat pump work input.

The upper theoretical value of COP is related to the Carnot cycle, which is:

$$COP_c = \frac{T_h}{T_h - T_c} \quad (19)$$

where $(T_h - T_c)$ is the temperature span over the distillation column.

For easy check the feasibility of using a heat pump in the distillation process, Plesu et al. [40] proposed a simplified equation for conceptual design:

$$COP_s = \frac{T_c}{T_R - T_c} \quad (20)$$

where T_R and T_c are temperature of reboiler and condenser, respectively. If $COP_s \geq 10$, the use of heat pump is recommended, if $5 < COP_s < 10$, it should be evaluated in more detail, and if $COP_s \leq 5$, using heat pump will not bring any benefits.

3. Process optimization

To perform simultaneous optimization of all the decision variables in each process configuration, a simulation-based optimization framework is developed, where process simulator Aspen Plus and external optimizer MATLAB are tightly linked to each other [41]. Initially, a combination of decision variables is randomly generated in MATLAB. Within each iteration, the decision variables are transferred into Aspen Plus, where the process simulator converges the flowsheet using the values from MATLAB. Then, the stream and process data required for the optimization is sent to MATLAB, where a population-based metaheuristic algorithm is performed. The optimization algorithm used in this work is a self-adapting dynamic differential evolution developed in our previous work [41]. The modified differential evolution is a global search optimization method suitable for difficult nonlinear/nonconvex MINLP problems. This iterative procedure continues until a specified termination criterion is met. In this study, the termination criterion is 300 generations, which is sufficient to obtain considerably good results based on our experiments. An optimization problem includes objective function and constraints. The objective function is the minimization of TAC, which is expressed in Eq. (6). The optimization constraints include product specifications and decision variable bounds.

For the THF/water separation, the product specifications are:

$$x_{B1}^{Water} \geq 0.9999 mol\% \quad (21)$$

$$x_{B2}^{THF} \geq 0.9999 mol\% \quad (22)$$

Table 2

The bound setting for each variable.

Decision variable	THF/water		Acetone/chloroform	
	Lower bound	Upper bound	Lower bound	Upper bound
N1	1	10	1	30
N2	0	5	1	30
N3	1	10	1	30
N4	1	20	1	30
N5	1	20	1	30
P _{T1} (bar)	0.45	1	5	15
P _{T2} (bar)	8	15	0.75	2
RR ₁	0	5	0	100
RR ₂	0	5	0	100
D ₂ /B ₂ (kmol/h)	60	115	450	650
T _{sup1} (°C)	0	20	0	40
T _{sup2} (°C)	0	20	0	40
P _{C1} (bar)	2	4	16	20
P _{C2} (bar)	18	20	1	4
FSR ₁	0	1	—	—
FSR ₂	0	1	—	—
PCS ₁	0.9	1	0.9	1
PCS ₂	0.9	1	0.9	1

For the acetone/chloroform separation, the product specifications are:

$$x_{D1}^{Acetone} \geq 0.995 mol\% \quad (23)$$

$$x_{D2}^{Chloroform} \geq 0.995 mol\% \quad (24)$$

On the other hand, lower and upper bounds are set for all discrete and continuous variables:

$$N^{min} \leq N \leq N^{max} \quad (25)$$

$$P_T^{min} \leq P_T \leq P_T^{max} \quad (26)$$

$$RR^{min} \leq RR \leq RR^{max} \quad (27)$$

$$D_2^{min} \leq D_2 \leq D_2^{max} \quad (28)$$

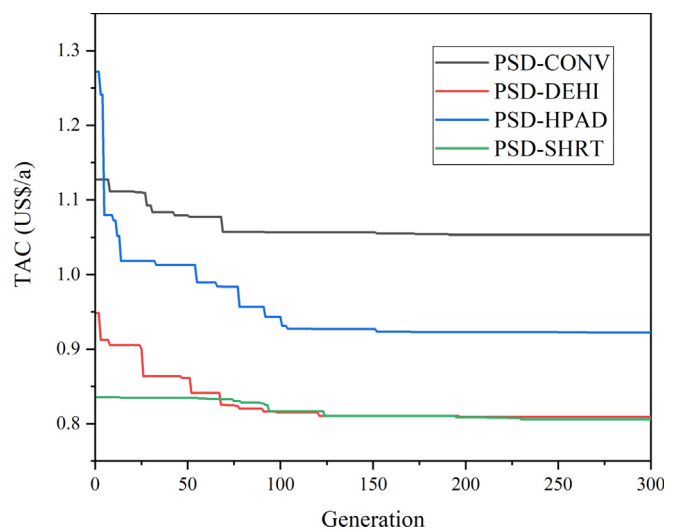


Fig. 12. The optimization progress curve for THF/water system.

Table 3

The optimum decision variables for THF/water system.

	PSD-CONV	PSD-DEHI	PSD-HPAD	PSD-SHRT
N1	9	10	9	10
N2	2	3	1	2
N3	2	2	2	3
N4	9	13	7	16
N5	14	10	13	14
P _{T1} (bar)	0.533	0.545	0.530	0.556
P _{T2} (bar)	12.70	12.74	12.06	11.97
RR ₁	0.16	0.11	0.14	0.16
RR ₂	0.60	0.67	0.71	0.67
D ₂ (kmol/h)	77.35	81.80	79.05	78.61
T _{sup1} (°C)	—	—	0.35	0.37
T _{sup2} (°C)	—	—	5.137	6.003
P _{C1} (bar)	—	—	2.731	2.905
P _{C2} (bar)	—	—	19.869	19.819
FSR ₁	—	—	—	0.176
FSR ₂	—	—	—	0.2
PCS ₁	—	—	—	1.0
PCS ₂	—	—	—	1.0

$$B_2^{\min} \leq B_2 \leq B_2^{\max} \quad (29)$$

$$T_{sup}^{min} \leq T_{sup} \leq T_{sup}^{max} \quad (30)$$

$$P_C^{min} \leq P_C \leq P_C^{max} \quad (31)$$

$$FSR^{min} \leq FSR \leq FSR^{max} \quad (32)$$

$$PCS^{min} \leq PCS \leq PCS^{max} \quad (33)$$

The bound settings for each variable are given in Table 2.

4. Results and discussions

4.1. THF/water separation

For the THF/water separation, based on the simulation-based optimization framework, the optimization progress curve for all the process configurations is given in Fig. 12. Table 3 provides all the final optimum decision variables that have been evolved for 300 generations. The optimum PSD-CONV, PSD-DEHI, PSD-HPAD, and PSD-SHRT, as well as their T-H composite curves and grand composite curves (GCCs) with a minimum temperature difference of 5 °C are demonstrated in Figs. 13–16, respectively. A thorough economic and environmental comparison of these optimum configurations is given in Table 4.

The optimum PSD-CONV displayed in Fig. 13a is used as the base case for comparisons. Note that its T-H and GCC diagrams (Fig. 13b and c) are almost identical to that of PSD-DEHI (Fig. 14b and c), illustrating the possibility of WHR through heat integration between HPC condenser (157.85°C) and LPC reboiler (87.19°C). However, in this case, the huge amount of waste heat in HPC overhead vapor is discarded in the condenser by cold utility without recovery, resulting in the LPC reboiler has to be fully thermal-driven by the steam utility. Compared to the other alternative processes, the huge energy loss causes very high OPEX, which strongly influences the final TAC and CO_2 emission. Whereas, for the rest of the configurations employing WHR measures, the OPEX, TAC and CO_2 emission are significantly decreased.

The PSD-DEHI improves the performance of the PSD-CONV by

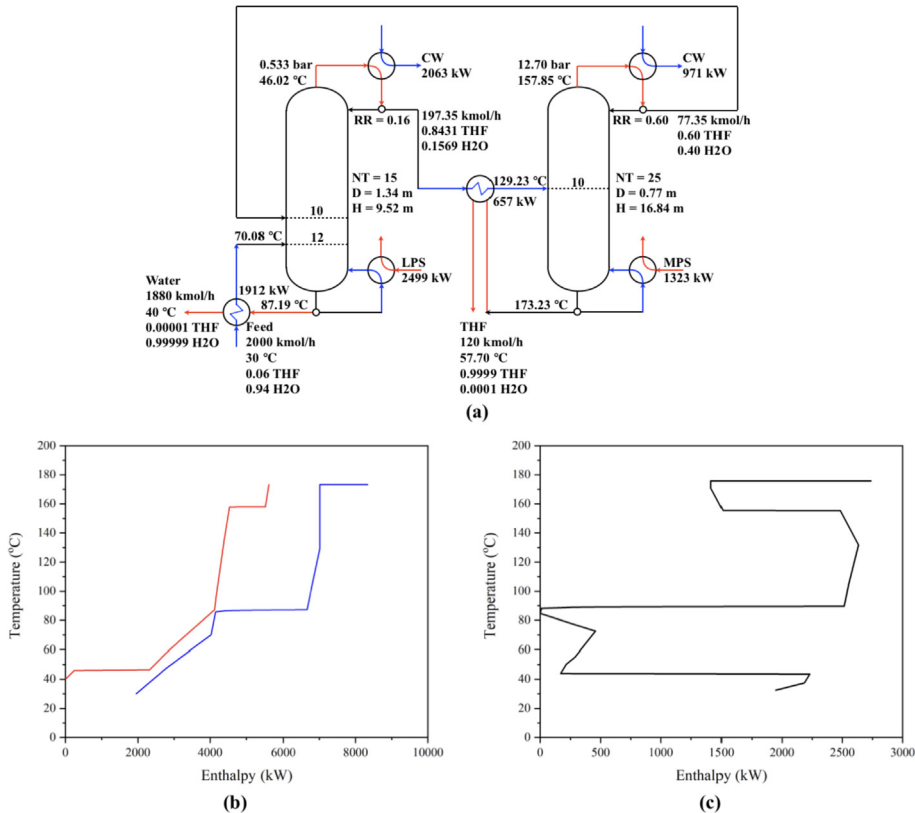


Fig. 13. (a) The optimum PSD-CONV for THF/water separation, (b) T-H composite curve, and (c) GCC.

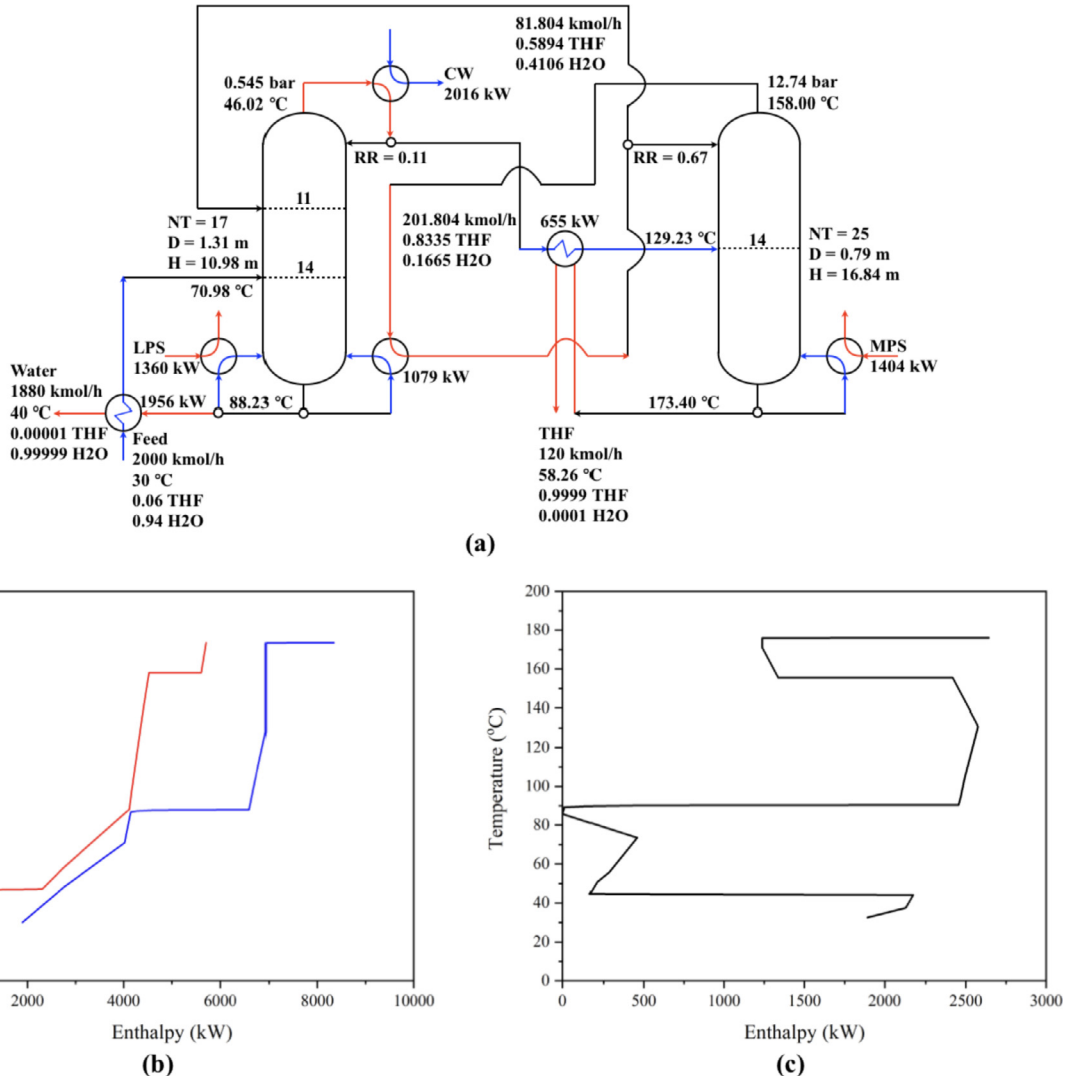


Fig. 14. (a) The optimum PSD-DEHI for THF/water separation, (b) T-H composite curve, and (c) GCC.

fully recovering waste heat in HPC overhead vapor. The resulting optimum configuration in Fig. 14a demonstrates PHI is more advantageous than FHI. In this manner, the OPEX is reduced by 27.26% at the expense of a slight CAPEX increase. Finally, the significant reduction in OPEX results in an overall 23.20% TAC reduction compared to the PSD-CONV. Besides, the CO₂ emission is also decreased by 27.07%, due to the less steam utility consumed.

Based on the result of the optimum PSD-CONV, the COP_s of the first and second column is 7.75 and 28.02, respectively. According to the feasibility equation proposed by Plesu et al. [40], the use of a heat pump needs to be evaluated in more detail. When the heat pump is introduced to the PSD, the HSCC on the T-H diagram is not only limited in the horizontal direction but shifts vertically to upgrade the waste heat sources that is originally condensed by the cold utility (Fig. 15b). Compared to the CSCC in processes that completely thermal-driven (Figs. 13b and 14b), the CSCC of PSD-

HPAD is almost maintained as it is, but the vertical movement in the HSCC makes it possible to circulate more energy within the system. However, constrained by the pinch point, the process still requires some steam utilities to compensate for the rest of energy consumption. Because of the involvement of two pricy compressors (the real heat pump COPs are 3.87 and 8.55), the significant increase of CAPEX makes it less competitive to the PSD-DEHI. However, the reduction of steam utility and the utilization of clean electrical power greatly reduce the CO₂ emission compared to the thermal-driven processes (PSD-CONV and PSD-DEHI).

When SHRT is incorporated into the design, the optimum results show the use of the cold utility can be completely eliminated. However, constrained by the pinch point, as shown in Fig. 16b, even the entire waste heat is upgraded and circulated, the HSCC still cannot fully cover the CSCC. So unlike the conventional SHRT column, this PSD-SHRT requires a small amount of steam utility

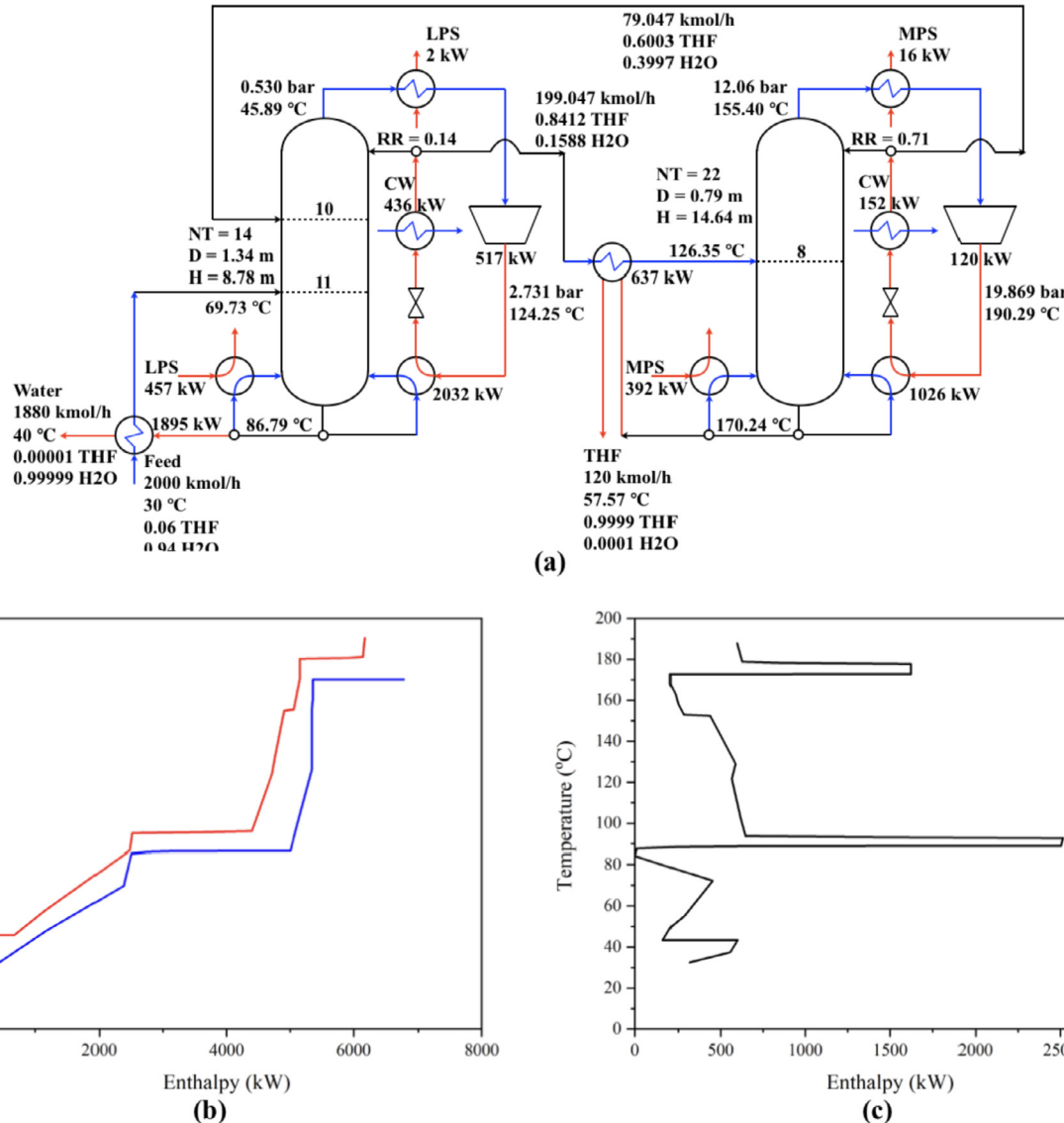


Fig. 15. (a) The optimum PSD-HPAD for THF/water separation, (b) T-H composite curve, and (c) GCC.

instead of completely driven by electricity. Compared to the PSD-HPAD, the PSD-SHRT requires more heat exchangers to recover sensible heat, so its CAPEX is higher than that of PSD-HPAD. However, the significant reduction of OPEX makes PSD-SHRT having the lowest TAC among all the design alternatives. Moreover, because this process is mainly driven by electricity, its CO₂ emission is also the lowest one. Compared to the thermal-driven PSD-CONV, PSD-SHRT reduces CO₂ emission by 83.67%.

4.2. Acetone/chloroform separation

For the acetone/chloroform separation, Fig. 17 shows the optimization progress curve, and Table 5 provides the final optimum decision variables for all processes. Under the minimum temperature difference of 5 °C, the optimum configurations, T-H composite curves, and GCCs of PSD-CONV, PSD-DEHI, PSD-HPAD, and PSD-SHRT are given in Figs. 18–21, respectively. The detailed economic

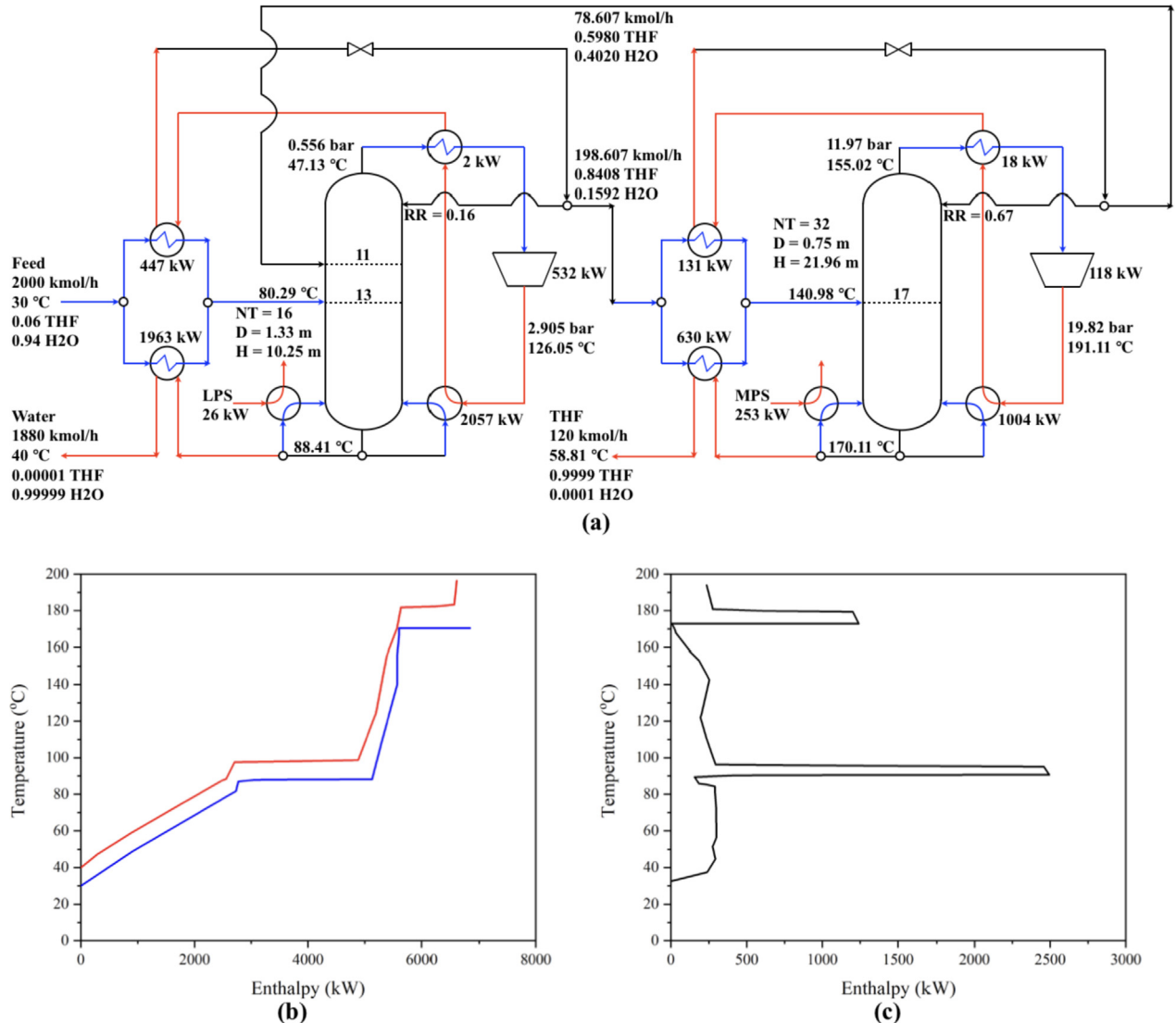


Fig. 16. (a) The optimum PSD-SHRT for THF/water separation, (b) T-H composite curve, and (c) GCC.

Table 4
Comparison of four process configurations for THF/water separation.

	PSD-CONV	PSD-DEHI	PSD-HPAD	PSD-SHRT
Cooling water duty (kW)	3034	2016	588	0
LPS steam duty (kW)	2499	1360	459	26
MPS steam duty (kW)	1323	1404	408	253
Total steam duty (kW)	3822	2764	867	279
Electrical power (kW)	0	0	637	650
OPEX (10 ⁶ US\$/a)	0.9040	0.6576	0.5136	0.3801
Total CAPEX (10 ⁶ US\$)	1.2746	1.2909	3.4804	3.6071
Annual CAPEX (10 ⁶ US\$/a)	0.1497	0.1516	0.4086	0.4237
TAC (10 ⁶ US\$/a)	1.0537	0.8092	0.9224	0.8038
OPEX/TAC ratio	0.8579	0.8127	0.5568	0.4729
TAC reduction	—	23.20%	12.46%	23.72%
CO ₂ emission (kg CO ₂ /h)	1356.7	989.5	427.0	221.5
CO ₂ emission reduction	—	27.07%	68.53%	83.67%

and environmental comparisons of these optimum processes are demonstrated in Table 6. It can be observed that the three improved schemes (PSD-DEHI, PSD-HPAD, and PSD-SHRT) have overwhelming advantages in economic and environmental aspects over the base case. Compared to the conventional design, the TAC of

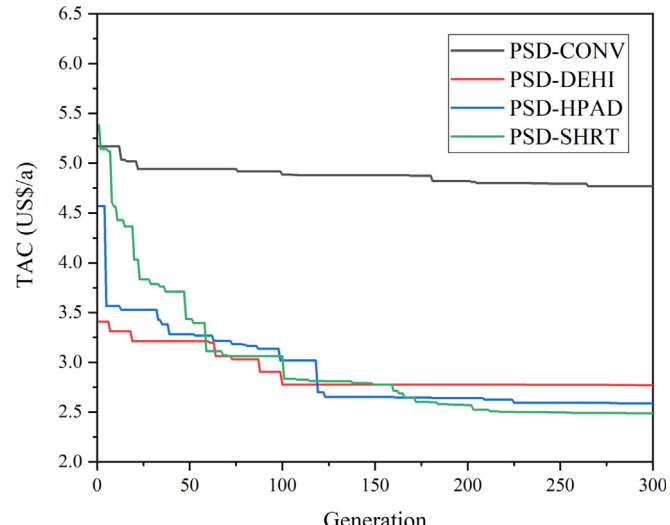


Fig. 17. The optimization progress curve for acetone/chloroform system.

Table 5

The optimum decision variables for acetone/chloroform system.

	PSD-CONV	PSD-DEHI	PSD-HPAD	PSD-SHRT
N1	20	20	14	16
N2	30	30	27	25
N3	30	30	9	26
N4	20	19	20	18
N5	21	23	16	12
P _{T1} (bar)	10.69	9.74	10.66	9.17
P _{T2} (bar)	0.75	0.75	0.85	0.75
RR ₁	27.63	26.24	33.90	28.17
RR ₂	19.81	21.85	20.21	22.51
B ₂ (kmol/h)	570.32	563.78	575.00	564.72
T _{sup1} (°C)	—	—	30.15	15.22
T _{sup2} (°C)	—	—	2.24	3.78
P _{C1} (bar)	—	—	16.08	17.39
P _{C2} (bar)	—	—	1.43	1.30
PCS ₁	—	—	—	1.0
PCS ₂	—	—	—	0.982

these improved processes are reduced by 41.92%, 45.50%, and 47.82%, respectively. And the CO₂ emissions are reduced by 45.73%, 85.84%, and 92.90%, respectively.

Applying WHR measures on the PSD-CONV can bring significant benefits to the overall process. Note that the T-H composite curve of PSD-CONV in Fig. 18 illustrates only PHI between HPC and LPC, but the simultaneous optimization results demonstrate the heat duty of the auxiliary reboiler approaches zero, so FHI is more advantageous. This FHI feature is shown in the pocket of PSD-DEHI GCC in Fig. 19c. For the use of FHI, the reduction of one heat exchanger makes the PSD-DEHI requiring less CAPEX compared to the conventional design. Besides, heat integration greatly reduces the OPEX and CO₂ emission caused by a steam utility. Although the PSD-DEHI can dramatically improve the process performance, it is still a thermal-driven process.

Based on the overhead and bottoms temperature of the PSD-CONV, the COP_s of the two columns are 26.58 and 24.19, which are greatly larger than 10, so the use of the heat pump is highly recommended. The simultaneous optimization results of PSD-HPAD show that the auxiliary reboilers are eliminated but the compressor preheaters still maintain, so this process can be

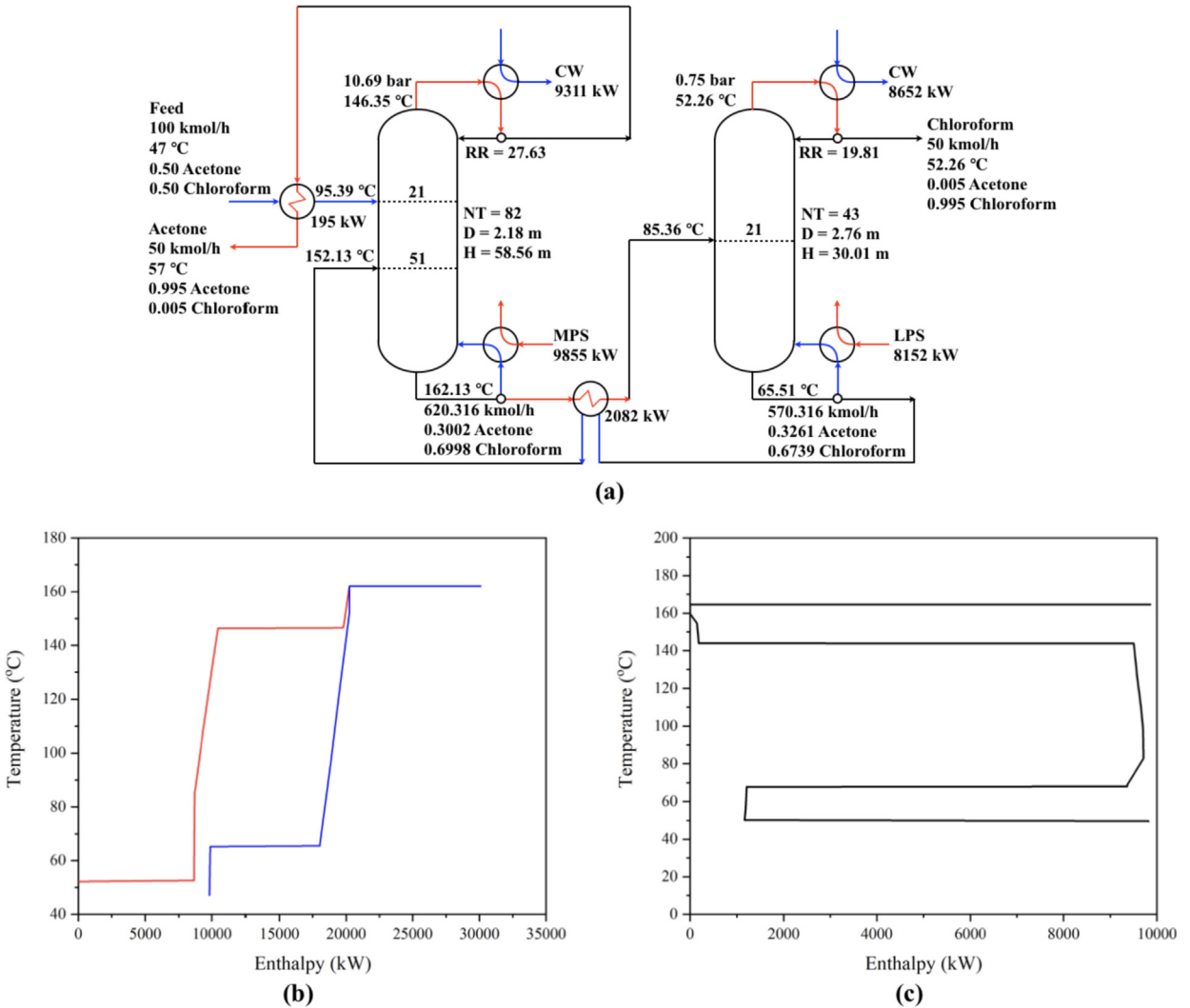


Fig. 18. The optimum PSD-CONV for acetone/chloroform separation, (b) T-H composite curve, and (c) GCC.

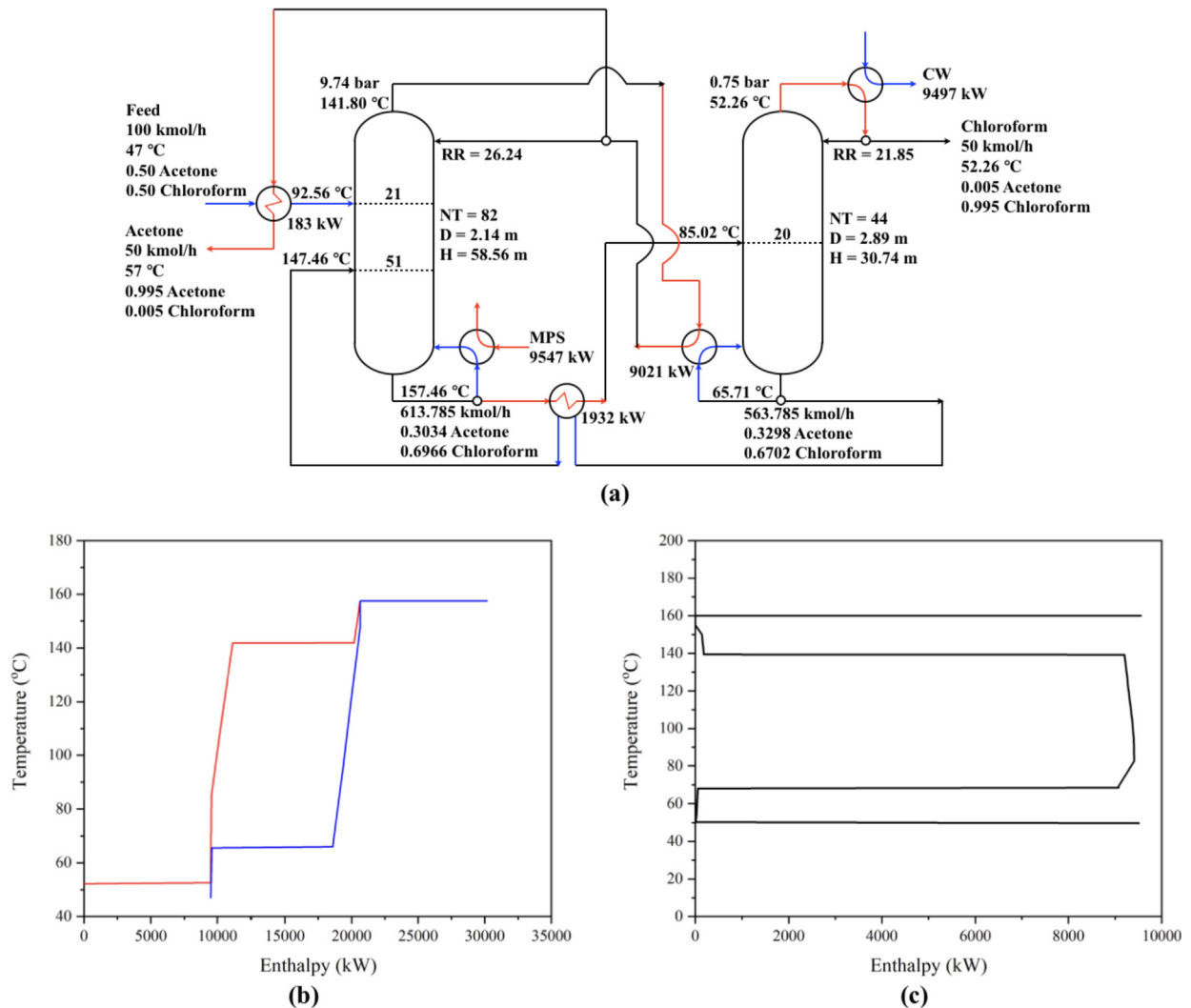


Fig. 19. The optimum PSD-DEHI for acetone/chloroform separation, (b) T-H composite curve, and (c) GCC.

regarded as a hybrid thermal-electrical-driven process, whose feature can be easily understood through analyzing the T-H composite curve (Fig. 20b). The calculated COP for each compressor is 9.06 and 11.12, respectively. The high COP in each heat pump significantly reduces OPEX and CO₂ emission compared to fully thermal-driven processes, indicating the great advantage of process electrification.

As a further improvement of the hybrid thermal-electrical-driven PSD-HPAD, the optimum PSD-SHRT configuration (Fig. 21a) shows the use of the hot utility can be completely eliminated,

so only electricity is input in the compressors to achieve heat circulation within the whole process. As demonstrated in the T-H composite curve (Fig. 21b), the HSCT is moved vertically to cover the entire CSCC, so the WHR is enhanced compared to the PSD-HPAD. It can be observed that with the aid of the SHRT, not only latent heat but also sensible heat are fully recovered. Referring to Table 6, the PSD-SHRT appears to be the configuration with the lowest TAC and CO₂ emission of all the alternative processes. These significant reductions in both TAC and CO₂ emission are mainly attributed to the reduction of reboiler duty, which is conventionally

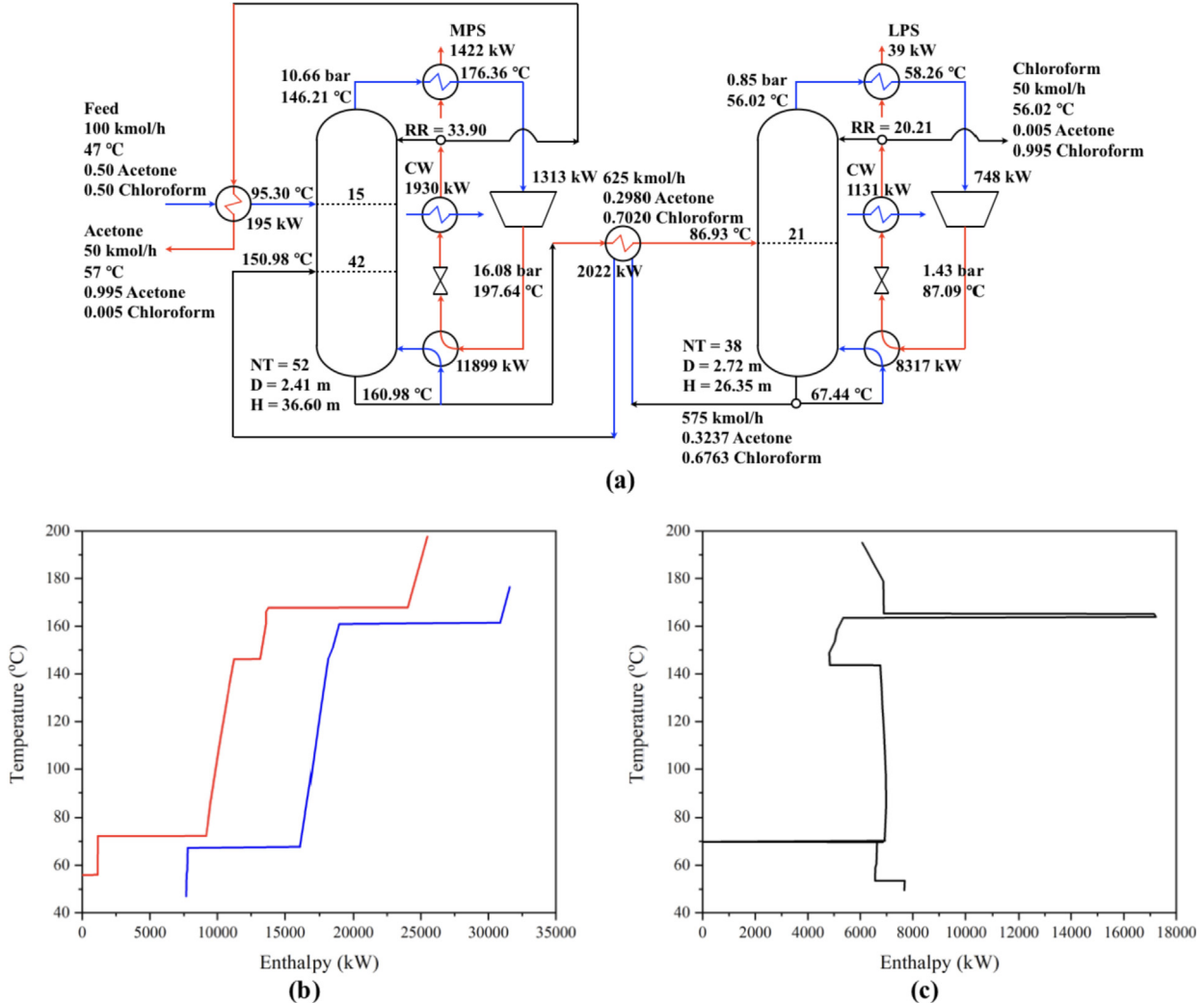


Fig. 20. The optimum PSD-HPAD for acetone/chloroform separation, (b) T-H composite curve, and (c) GCC.

thermal-driven. Also, since the PSD-SHRT process can be completely electrical-driven in steady-state mode, it is possible to use renewable energy sources instead of fossil fuel combustion to further improve plant sustainability.

5. Conclusions

This study describes process electrification through simultaneous optimization methodology to intensify the cost-intensive azeotropic separation by PSD. The electric-driven PSD-SHRT is compared with three other alternative processes (PSD-CONV, PSD-DEHI, and PSD-HPAD) in terms of their capability to conserve

process cost and CO₂ emission. For cases of minimum/maximum-boiling azeotropes (THF/water and acetone/chloroform), significant cost reduction is observed and environmental benefit achieved using the SHRTs. Amongst the four options, PSD-SHRT stands out with the lowest TAC and CO₂ emission. The PSD-SHRT for THF/water system wins PSD-CONV by 23.72% for TAC and 83.67% for CO₂ emissions, respectively. These corresponding superiorities increase to 47.82% and 92.90% for the acetone/chloroform system. These results indicate the great advantages of electric-driven over thermal-driven in reducing process cost and CO₂ emission. Therefore, PSD-SHRT is highly recommended to other pressure-sensitive azeotropic systems. Moreover, the concept of process electrification

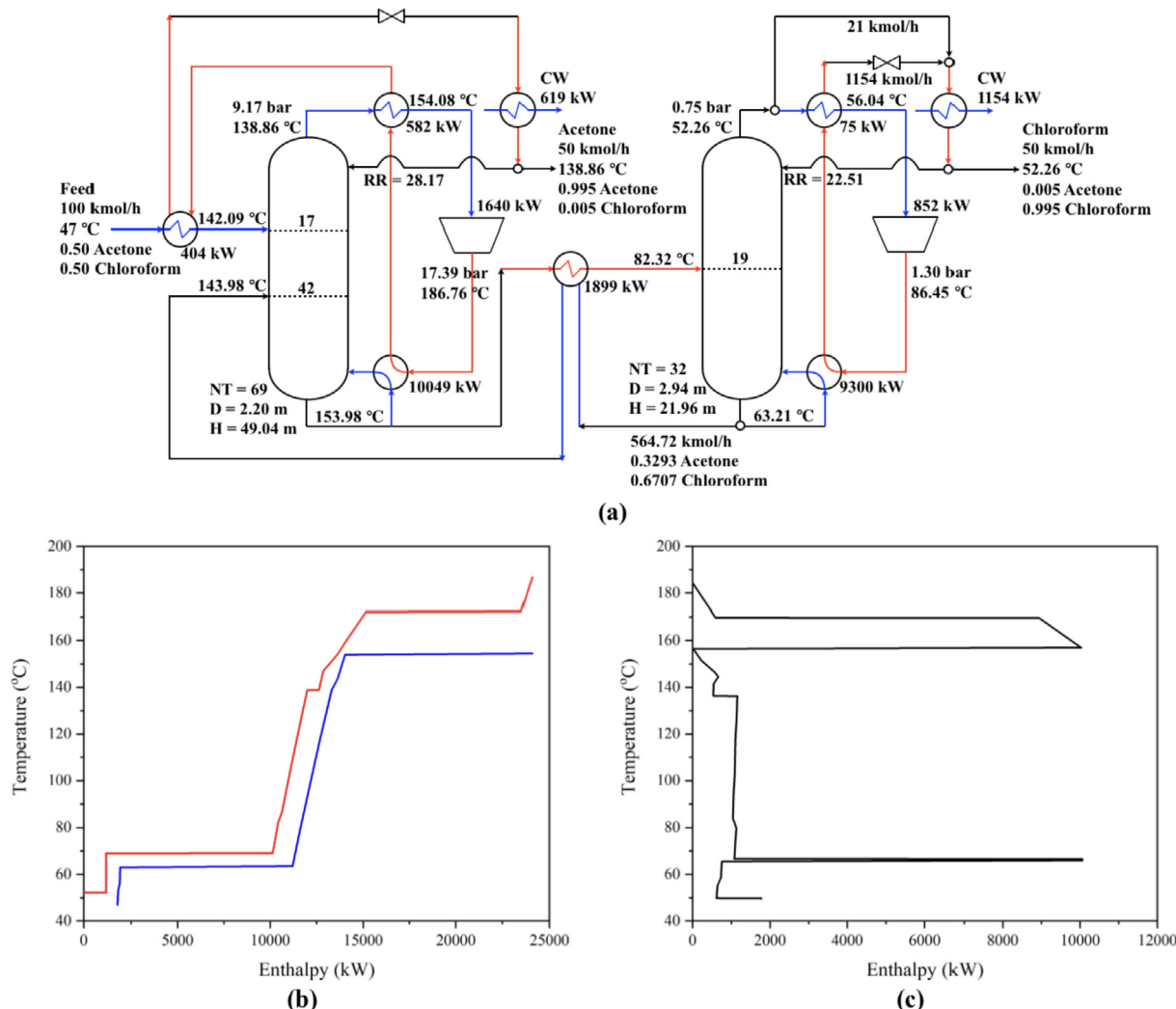


Fig. 21. The optimum PSD-SHRT for acetone/chloroform separation, (b) T-H composite curve, and (c) GCC.

Table 6
Comparison of four process configurations for acetone/chloroform separation.

	PSD-CONV	PSD-DEHI	PSD-HPAD	PSD-SHRT
Cooling water duty (kW)	17963	9497	3061	1773
LPS steam duty (kW)	8152	0	39	0
MPS steam duty (kW)	9855	9547	1422	0
Total steam duty (kW)	18007	9547	1461	0
Electrical power (kW)	0	0	2061	2492
OPEX (10^6 US\$/a)	4.3427	2.3570	1.3738	1.2235
Total CAPEX (10^6 US\$)	3.6368	3.5205	10.4357	10.7746
Annual CAPEX (10^6 US\$/a)	0.4272	0.4135	1.2258	1.2656
TAC (10^6 US\$/a)	4.7699	2.7705	2.5996	2.4891
OPEX/TAC ratio	0.9104	0.8507	0.5285	0.4915
TAC reduction	—	41.92%	45.50%	47.82%
CO ₂ emission (kg CO ₂ /h)	6459.6	3505.7	914.9	458.4
CO ₂ emission reduction	—	45.73%	85.84%	92.90%

is worth to extend to other distillation processes.

Acknowledgements

This work was supported by the Basic Science Research Program through the National Research Foundation of Korea (NRF) funded by the Ministry of Education (2018R1A2B6001566), and by Priority

Research Center Program through the National Research Foundation of Korea (NRF) funded by the Ministry of Education (2014R1A6A1031189). In addition, the authors thank the China-ASEAN Scholar Program sponsored through Tianjin University funded by the Belt and Road Expert Introduction Program (G20190002046).

References

- [1] Kiss AA, Bildea CS. A control perspective on process intensification in dividing wall columns. *Chem Eng Process Process Intensif* 2011;50:281–92.
- [2] Matsuda K, Kansha Y, Fushimi C, Tsutsumi A, Kishimoto A. Advanced energy saving and its applications in industry. London: Springer; 2013.
- [3] Luyben WL, Chien IL. Design and control of distillation systems for separating azeotropes. Wiley; 2010.
- [4] Luyben WL. Design and control of a fully heat-integrated pressure-swing azeotropic distillation system. *Ind Eng Chem Res* 2008;47:2681–95.
- [5] Cui C, Li X, Sui H, Sun J. Optimization of coal-based methanol distillation scheme using process superstructure method to maximize energy efficiency. *Energy* 2017;119:110–20.
- [6] Cui C, Li X, Guo D, Sun J. Towards energy efficient styrene distillation scheme: from grassroots design to retrofit. *Energy* 2017;134:193–205.
- [7] Cui C, Xi Z, Liu S, Sun J. An enumeration-based synthesis framework for multi-effect distillation processes. *Chem Eng Res Des* 2019;144:216–27.
- [8] Kiss AA, Landaeta SJF, Ferreira CAL. Towards energy efficient distillation technologies – making the right choice. *Energy* 2012;47:531–42.
- [9] Long NVD, Lee M. Review of retrofitting distillation columns using thermally coupled distillation sequences and dividing wall columns to improve energy

- efficiency. *J Chem Eng Jpn* 2014;47:87–108.
- [10] Leo MB, Dutta A, Farooq S. Process synthesis and optimization of heat pump assisted distillation for ethylene-ethane separation. *Ind Eng Chem Res* 2018;57:11747–56.
 - [11] Li X, Geng X, Cui P, Yang J, Zhu Z, Wang Y, Xu D. Thermodynamic efficiency enhancement of pressure-swing distillation process via heat integration and heat pump technology. *Appl Them Eng* 2019;154:519–29.
 - [12] Jain S, Smith R, Kim JK. Synthesis of heat-integrated distillation sequence systems. *J Taiwan Inst Chem Eng* 2012;43:525–34.
 - [13] Li X, Cui C, Li H, Gao X. Process synthesis and simultaneous optimization of extractive distillation system integrated with organic Rankine cycle and economizer for waste heat recovery. *J Taiwan Inst Chem Eng* 2019;102: 61–72.
 - [14] Kemp IC. Pinch analysis and process integration: a user guide on process integration for the efficient use of energy. Elsevier; 2007.
 - [15] Chen Y, Eslick JC, Grossmann IE, Miller DC. Simultaneous process optimization and heat integration based on rigorous process simulations. *Comput Chem Eng* 2015;81:180–99.
 - [16] Kansha Y, Tsuru N, Sato K, Fushimi C, Tsutsumi A. Self-heat recuperation technology for energy saving in chemical processes. *Ind Eng Chem Res* 2009;48:7682–6.
 - [17] Long NVD, Lee M. A novel NGL (natural gas liquid) recovery process based on self-heat recuperation. *Energy* 2013;57:663–70.
 - [18] Matsuda K, Kawazuishi K, Kansha Y, Fushimi C, Nagao M, Kunikiyo H, Masusa F, Tsutsumi A. Advanced energy saving in distillation process with self-heat recuperation technology. *Energy* 2011;36:4640–5.
 - [19] Kansha Y, Kishimoto A, Tsutsumi A. Application of the self-heat recuperation technology to crude oil distillation. *Appl Them Eng* 2012;43:153–7.
 - [20] Fu Q, Song C, Kansha Y, Liu Y, Ishizuka M, Tsutsumi A. Energy saving in a biodiesel production process based on self-heat recuperation technology. *Chem Eng J* 2015;278:556–62.
 - [21] Kansha Y, Kishimoto A, Nakagawa T, Tsutsumi A. A novel cryogenic air separation process based on self-heat recuperation. *Separ Purif Technol* 2011;77: 389–96.
 - [22] Long NVD, Lee M. Novel acid gas removal process based on self-heat recuperation technology. *Int J Greenh Gas Contr* 2017;64:34–42.
 - [23] Kansha Y, Tsuru N, Fushimi C, Tsutsumi A. New design methodology based on self-heat recuperation for production by azeotropic distillation. *Energy Fuels* 2010;24:6099–102.
 - [24] Xia H, Ye Q, Feng S, Li R, Suo X. A novel energy-saving pressure swing distillation process based on self-heat recuperation technology. *Energy* 2017;141:770–81.
 - [25] Luyben WL. Distillation column pressure selection. *Separ Purif Technol* 2016; 62–7.
 - [26] Cui C, Liu S, Sun J. Optimal selection of operating pressure for distillation columns. *Chem Eng Res Des* 2018;137:291–307.
 - [27] Cui C, Sun J. Rigorous design and simultaneous optimization of extractive distillation systems considering the effect of column pressures. *Chem Eng Process Process Intensif* 2019;139:68–77.
 - [28] Christopher CCN, Dutta A, Farooq S, Karimi IA. Process synthesis and optimization of propylene/propane separation using vapor recompression and self-heat recuperation. *Ind Eng Chem Res* 2017;56:14557–64.
 - [29] Li X, Cui C, Li H, Gao X. Process synthesis and simulation-based optimization of ethylbenzene/styrene separation using double-effect heat integration and self-heat recuperation technology: a techno-economic analysis. *Separ Purif Technol* 2019;228:115760.
 - [30] Abu-Elshah SI, Luyben WL. Design and control of a two-column azeotropic distillation system. *Ind Eng Chem Process Des Dev* 1985;24:129–32.
 - [31] Luyben WL. Comparison of flowsheets for THF/water separation using pressure-swing distillation. *Comput Chem Eng* 2018;115:407–11.
 - [32] Luyben WL. Comparison of extractive distillation and pressure-swing distillation for acetone/chloroform separation. *Comput Chem Eng* 2013;50:1–7.
 - [33] Cui C, Li X, Sui H, Sun J. Quick decision-making for close-boiling distillation schemes. *Ind Eng Chem Res* 2017;56:5078–91.
 - [34] Kiss AA. Advanced distillation technologies: design, control and applications. Wiley; 2013.
 - [35] Smith R. Chemical process design and integration. Wiley; 2005.
 - [36] Luyben WL. Principles and case studies of simultaneous design. Wiley; 2011.
 - [37] Gadalla MA, Olujic Z, Jansens PJ, Jobson M, Smith R. Reducing CO₂ emissions and energy consumption of heat-integrated distillation systems. *Environ Sci Technol* 2005;39:6860–70.
 - [38] Smith JM, Van Ness HC, Abbott MM. Introduction to chemical engineering thermodynamics. McGraw-Hill; 1996.
 - [39] Waheed MA, Oni AO, Adejuwogbe SB, Adewumi BA, Fadare DA. Performance enhancement of vapor recompression heat pump. *Appl Energy* 2014;114: 69–79.
 - [40] Plesu V, Bonet-Ruiz AE, Bonet J, Llorens J. Simple equation for suitability of heat pump use in distillation. *Comput Aid Chem Eng* 2014;33:1327–32.
 - [41] Cui C, Zhang X, Sun J. Design and optimization of energy-efficient liquid-only side-stream distillation configurations using a stochastic algorithm. *Chem Eng Res Des* 2019;145:48–52.